Received: 11 March 2019 | Revised: 21 July 2020 | Accepted: 24 July 2020
DOI: 10.1111/bph.15239

RESEARCH PAPER

Effects of a monocarboxylate transport 1 inhibitor, AZD3965, on retinal and visual function in the rat

Annette E. Allen[1] | Elizabeth A. Martin[2] | Katherine Greenwood[2,3] | Claire Grant[2] | Peter Vince[2] | Robert J. Lucas[1] | William S. Redfern[2,4]

[1]Faculty of Biology, Medicine and Health, University of Manchester, Manchester, UK
[2]Regulatory Safety Centre of Excellence, Clinical Pharmacology & Safety Sciences, BioPharmaceuticals R&D, AstraZeneca, Cambridge, UK
[3]Gentronix Limited, Cheshire, UK
[4]Certara UK Limited, Sheffield, UK

Correspondence
Dr. Elizabeth Martin, Regulatory Safety Centre of Excellence, Clinical Pharmacology & Safety Sciences, BioPharmaceuticals R&D, AstraZeneca, Cambridge, UK
Email: elizabeth.martin@astrazeneca.com

Present address
Elizabeth A. Martin, Drug Safety & Metabolism IMED Biotech Unit, AstraZeneca, Melbourne Science Park, Hertfordshire SG8 6HB, UK.

Background and Purpose: Inhibition of monocarboxylate transport 1 (MCT1) is of interest in targeting highly glycolytic tumours. However, MCT1 is expressed in retina, and so inhibition of MCT1 could affect retinal function.

Experimental Approach: AZD3965, an MCT1 inhibitor selected for clinical development, and two additional MCT1 inhibitors were evaluated for effects on visual acuity in albino (Han Wistar) rats. The effects of AZD3965 on visual acuity and electroretinography (ERG) were further investigated in pigmented (Long-Evans) rats, with dosing for up to 7 days.

Key Results: All three MCT1 inhibitors reduced visual acuity within 2 h of dosing, suggesting a class effect. The deficit caused by AZD3965 (1,000 mg·kg^{-1} p.o. per day for 4 days) in Long Evans rats recovered to pre-dose levels 7 days after cessation of dosing. AZD3965 (50 to 1,000 mg·kg^{-1} p.o.) reduced the amplitude of scotopic a- and b-waves, and photopic b-wave of the ERG in a dose-related fashion, within 2 h of dosing. The effects on the scotopic ERG had diminished by Day 7 of dosing, demonstrating partial restoration of function despite continued treatment. Seven days after cessation of dosing at the highest dose tested (1,000 mg·kg^{-1}), there was recovery of both scotopic a- and b- waves and, to a lesser extent, photopic b-wave. ERG was affected at lower plasma exposures than was visual function.

Conclusions and Implications: This study clarifies the role of the MCT1 transporter in retinal function. The monitorability of the functional effects on the retina enabled safe clinical use of AZD3965.

KEYWORDS
AZD3965, ERG, MCT1, rat, retina, visual acuity

1 | INTRODUCTION

Monocarboxylates such as lactate and pyruvate underpin many aspects of cellular metabolism and cell communication. The transport of these short-chain carbon molecules across the plasma membrane is thus essential for numerous physiological functions and is mediated by a family of monocarboxylate transporters (SLC16) or MCTs. Currently, there are known to be 14 MCT (SLA16A1-14) subtypes (Halestrap & Meredith, 2004), though only subtypes 1–4 (MCT1–4) are understood at present to partake in bi-directional proton-linked monocarboxylate transport (Bröer et al., 1998; Bröer et al., 1999; Grollman, Philp, McPhie, Ward, & Sauer, 2000; Manning Fox, Meredith, & Halestrap, 2000). MCT1–4 are expressed to varying degrees in

Abbreviations: ERG, electroretinogram; MCT, monocarboxylate transporter; T_{max}, time of maximal plasma concentration.

many tissues including skeletal muscle, cardiac tissue, brain and retina (see Halestrap & Price, 1999, for a comprehensive summary) and, as such, facilitate diverse biological functions.

Recently, MCTs have been considered as a potential pharmacological target for the suppression of tumour growth, in which there is a reliance on MCTs for lactate-fuelled respiration (Clem, O'Neal, Klarer, Telangand, & Chesney, 2016; Doherty & Cleveland, 2013; Jones & Morris, 2016; Martinez-Outschoorn, Peiris-Pagès, Pesstell, Sotgia, & Lisanti, 2017; Ross & Critchlow, 2014; Selwan, Finicle, Kim, & Edinger, 2016; Sonveaux et al., 2008). Because of a limited oxygen supply, hypoxic cells deep within a tumour rely on glycolytic metabolism to meet their energy demands. The end product, lactate, is ultimately secreted via MCT4 transporters to the interstitial fluid. Oxygenated cells in the tumour periphery express MCT1 transporters to enable the uptake of this lactate which, following conversion to pyruvate by lactic acid dehydrogenase (B LDH-B), is used as a substrate for oxidative metabolism. This symbiotic relationship maintains energy homeostasis in oxygenated and hypoxic tumour cells and is reliant on MCT1 transport of lactate. Accordingly, the therapeutic potential for MCT1 inhibitors has recently been demonstrated, whereby inhibition of MCT1 transport with siRNA or α-cyano-4-hydroxycinnamate (a reversible nonselective inhibitor of MCTs (Halestrap & Denton, 1975; Manning Fox et al., 2000) suppresses lactate-fuelled respiration in tumour cells, delaying tumour growth and inducing tumour necrosis (Sonveaux et al., 2008). Hence, MCT1 inhibitors provide a realistic opportunity in the clinical treatment of tumours.

What is already known

- Monocarboxylate transporter 1 (MCT1) is present in the retina.
- Intravitreal injections nonselective MCT inhibitors (4-hydroxycinnamate and probenecid) affects electroretinogram (ERG) in rats.

What does this study add

- Three MCT1 inhibitors (including AZD3965) reduced visual acuity within 2 h of dosing in rats.
- AZD3965 affected the ERG in the rat, but the effects diminished on repeated dosing.

What is the clinical significance

- The monitorability of these retinal functional effects enabled safe clinical use of AZD3965.
- Recently published clinical data on AZD3965 confirmed translation to similar effects on the human ERG.

Given our knowledge of MCT expression throughout the body, MCT1 inhibitors must also be considered in terms of their effects on wider physiology. One area of potential concern is the retina, where MCT subtypes have been localised to almost every type of retinal neurone and the retinal pigment epithelium (Bergersen et al., 1999; Chidlow, Wood, Graham, & Osborne, 2005; Gerhart, Leino, & Drewes, 1999; Hosoya et al., 2001; Philp, Wang, Yoon, & Hjelmeland, 2003; Reichart & Strauss, 2014) and where monocarboxylate mobility is especially vital for neuronal function and signal transduction (Bui, Kalloniatis, & Vingrys, 2004; Bui, Vingrys, Wellard, & Kalloniatis, 2004; Zeevalk & Nicklas, 2000). The high metabolic rate within the retina is maintained chiefly by glycolysis, so that the major product of glucose metabolism is lactate, not CO_2 (Ames, Li, Heher, & Kimble, 1992; Wang, Kondo, & Bill, 1997; Wang, Tornquist, & Bill, 1997; Winkler, 1981). Moreover, lactate produced and released by Müller cells (retinal glial cells) has been suggested to fuel oxidative respiration in photoreceptors, bipolar cells and retinal ganglion cells, a process termed the "lactate shuttle" (Poitry-Yamate, Poitry, & Tsacopoulos, 1995; Tsacopoulos & Magistretti, 1996; Tsacopoulos, Poitry-Yamate, MacLeish, & Poitry, 1998; Pellerin, 2003; although see Winkler, Pourcho, Starnes, Slocum, & Slocum, 2003 for evidence of preferential use of glucose as a metabolic fuel by retinal neurones). These processes therefore require efficient lactate transfer between retinal neurons and Müller cells, relying on functional MCTs. These processes may also lead to excess interstitial lactate, which requires removal to the choroidal circulation via the retinal pigment epithelium. MCT1 and MCT3 transporters located to the apical and basal membranes of the retinal pigment epithelium, respectively, are crucial in mediating this process (Gerhart et al., 1999; Kenyon, Yu, La Cour, & Miller, 1994; Lin, La Cour, Andersen, & Miller, 1994; Philp et al., 2003; Philp, Yoon, & Grollman, 1998; Reichart & Strauss, 2014). The monocarboxylate pyruvate is also an essential component of metabolic pathways in the retina. MCTs enable pyruvate to enter the tricarboxylic acid cycle within the mitochondria, thus combining glycolytic and oxidative metabolism in retinal neurons. In addition, the tricarboxylic acid cycle is also responsible for the production of an important intermediate, α-ketoglutarate, which together with ammonium ions synthesises the retina's principal neurotransmitter, glutamate (Erecinska & Silver, 1990).

Put together, it is clear that many aspects of retinal physiology require MCTs to maintain sufficient energy metabolism and also neurotransmitter synthesis. It is perhaps unsurprising then that the nonselective MCT inhibitor 4-hydroxycinnamate results in both a reduction in ATP metabolism and in retinal glutamate production (Zeevalk & Nicklas, 2000). Intravitreally injected 4-hydroxycinnamate (and also another non-selective MCT inhibitor, probenecid) causes a significant decrease in the amplitude of the electroretinogram (ERG) b-wave, indicating a reduction in retinal ON bipolar cell functionality (Bui, Kalloniatis, & Vingrys, 2004; Bui, Vingrys, et al., 2004).

Clearly, MCTs have a vital role in the retina. However, it is not currently understood how inhibition of specific MCT subtypes, including MCT1, might influence vision. Retinal MCT1 expression has been identified specifically within Müller cells, photoreceptor inner segments, the inner blood-retinal barrier and the apical and basal membranes of the retinal pigment epithelium (Bergersen et al., 1999; Chidlow et al., 2005; Gerhart et al., 1999; Hosoya et al., 2001; Philp et al., 2003; Reichart & Strauss, 2014) and so it is conceivable that MCT1 inhibition will have measurable effects on retinal function. This is an important consideration if MCT1 inhibitors are to be developed for tumour therapy. Moreover, it is currently unclear whether these effects are fully or partially reversible and/or whether these effects would be cumulative with repeated dosing. Thus, to ascertain the effects of MCT1 inhibition within the retina, we measured the effects of three MCT1 inhibitors (AZD3965, AZ11709220 and AR-C117977XX) on visual function in albino rats using an optomotor reflex method (Douglas et al., 2005; Prusky, Alam, Beekman, & Douglas, 2004; Redfern et al., 2011). **AZD3965** is selective for MCT1 (nanomolar potency) over MCT4 (inactive at 10 μM), with sixfold selectivity over MCT2 (Curtis et al., 2017) and was selected for development as a first-in-class oncology agent to treat advanced solid tumours (Clem et al., 2016; Doherty & Cleveland, 2013; Jones & Morris, 2016; Martinez-Outschoorn et al., 2017; Polanski et al., 2014; Ross & Critchlow, 2014; Selwan et al., 2016). AR-C117977XX has been previously described (compound 1 in Murray et al., 2005; Påhlman et al., 2012). We subsequently evaluated the effects of AZD3965 on visual acuity and on the electroretinogram (ERG) in pigmented rats. The ERG provides a reliable assessment of broad-scale retinal function, with the a- and b-waves indicating photoreceptor and second-order cell responses, respectively, and thereby is a useful tool in assessing any deficits in outer-retinal function (Rosolen, Rigaudiere, Le Gargasson, & Brigell, 2005).

AZD3965 has subsequently been tested in oncology patients with monitoring of ERG and visual function (Cancer Research, 2013; Plummer et al., 2017), so we now have an opportunity to assess pharmacological translation of its effects on ERG and visual acuity from rat to human.

2 | METHODS

2.1 | Ethical statement

The use of animals was kept to an absolute minimum required to achieve adequate statistical power. Animal studies are reported in compliance with the ARRIVE guidelines (Percie du Sert et al., 2020) and with the recommendations made by the *British Journal of Pharmacology* (Lilley et al., 2020). All procedures were conducted in accordance with the United Kingdom Animal (Scientific Procedures) Act 1986, approved by institutional ethical review committees (Alderley Park Animal Welfare and Ethical Review Board) and conducted under the authority of the Project Licence (40/3729). All animal facilities had been approved by the United Kingdom Home Office Licensing Authority and met all current regulations and standards of the United Kingdom.

2.2 | Overall strategy

Han Wistar rats were the preferred strain for toxicology and safety pharmacology studies in AstraZeneca and so were the default choice to use for an initial assessment of potential effects of these compounds on visual acuity. However, as an albino strain, they are less suitable for ERG recordings due to inherent deficiencies in the albino visual system, including lower amplitudes of the ERG waveform. Therefore, a pigmented strain (Long Evans) was used for more detailed evaluation of the compound of interest, AZD3965. This strain is more difficult to source routinely so was not used for visual acuity testing of the other two compounds. Separate groups of Long Evans rats were used for visual acuity and ERG recordings. Therefore, the overall strategy comprised a three-tiered approach:- (a) establish whether each of three MCT1 inhibitors would cause a deficit in visual acuity in Han Wistar rats after a single dose, (b) investigate the effects of the compound selected for clinical development (AZD3965) on visual acuity in Long Evans rats using once daily repeated dosing and (c) evaluate the effects of AZD3965 on retinal function using ERG in Long Evans rats, including the effects of repeat dosing and post-dose recovery.

2.3 | Animals, housing and husbandry

Male and female Han Wistar rats (189–298 g; 8–10 weeks of age, at time of dosing) were used for visual acuity measurements on the three MCT1 inhibitors. Male and female Long Evans hooded rats (188–260 g; 7–9 weeks old at start of dosing) were used for visual acuity measurements on AZD3965, while male Long Evans hooded rats (120–327 g; 5–6 weeks old at start of dosing) were used for ERG recordings.

Han Wistar rats were obtained from Charles River Laboratories in Margate, Kent, UK (HsdHan:WIST; AZD3965 and AZ11709220 studies) or from Alderley Park Biological Services 1 (AlpkHsdRccHan:WIST; AR-C117977XX study); Long Evans rats (LE/CpbHsd) were obtained from Charles River Germany. Vendor-supplied health reports indicated that the rats were free of known viral, bacterial and parasitic pathogens. The animals were kept in groups of four to five in transparent plastic cages, with floor space measuring approximately 59 × 38 cm, placed in racks in a 12 h light: dark cycle. Target values for temperature and relative humidity were 19°C to 23°C and 40% to 70%, respectively. Recorded values were within these limits throughout the housing period required for the study. The cages contained a layer of Aspen chip bedding together with environmental enrichment (sizzlenest nesting material, Datesand) medium Aspen brick chew sticks (Datesand) and a red plastic play tunnel. The rats had access to food (RM1E pelleted diet, Special Diet Services, UK) and water from the site drinking water supply ad libitum. Animals were allocated to cages/treatment groups on day of arrival according to study design and remained in the same social group throughout the study. The body weights were balanced evenly between groups. The rats were identified by waterproof tail markings. Each cage housed animals from one treatment group only. Rats were test-naïve prior to the studies. Animal welfare was assessed throughout by daily monitoring of appearance, behaviour and cage environment. Rats were allowed to acclimatise to the animal unit for at least 1 week before dosing.

2.4 | Visual acuity measurements

The principle of the OptoMotry system (Cerebral Mechanics Inc., Lethbridge, Alberta, Canada) is to measure visual acuity in rodents by determining the maximum grating frequency the animals can resolve. The method is essentially a virtual optomotor task for rapidly assessing visual acuity in conscious, unrestrained rodents (Douglas et al., 2005; Prusky et al., 2004; Redfern et al., 2011). The chamber comprises four 19″ computer monitors displaying vertical sinusoidal gratings with the animal's viewpoint at the centre of a “virtual cylinder.” Screen luminance was factory pre-set to equalise the screen intensity (black mean, 0.22 cd·m^{-2}; white mean, 152.13 cd·m^{-2}; Prusky et al., 2004). Contrast was set to the default value of 100%. The animal is placed inside the chamber on a platform and a video camera above the animal relays images onto a desktop computer screen, whereby a trained observer maintains the centre of the virtual cylinder on the head of the animal by repeatedly positioning a cross between the eyes on the video image using a computer mouse. The grating is rotated at 12° per second (2 rpm) to elicit head-tracking movements in the same direction as the visual motion. The observer selects “Yes” or “No” depending on whether the animal is observed to be making any characteristic head-tracking movements to follow the moving gratings. The grating frequency is progressively increased using a simple staircase method until there are no discernible head-tracking movements and the visual acuity threshold (in cycles per degree; c/d) of the animal is defined as the highest grating frequency which the animal responds to. Animals were habituated individually to the OptoMotry chamber for a short period of time prior to pre-study measurements with the aim of reducing activity levels on test days. On the days of assessment, animals were tested one at a time in the OptoMotry chamber. The number of times the cross was repositioned in the first 60 s of the animal being placed in the OptoMotry chamber was counted and recorded, as a measure of activity, to check that any apparent changes in visual acuity were not due to changes in behaviour or in the level of arousal. (This was not done in the case of AR-C117977XX as this compound was tested prior to our introduction of routine evaluation of activity in OptoMotry studies.)

2.5 | Electroretinography (ERG)

Recording of ERG is a non-surgical procedure which requires general anaesthesia to immobilise the animals. Also, rats have to be dark-adapted for at least 2 hours prior to the recording, to optimise functioning of the rod photoreceptors. Therefore, on recording days, rats were dosed in ambient room light 2 h prior to ERG recording, then immediately placed in complete darkness in a light-proofed ante-room adjacent to the ERG laboratory until transfer to the ERG laboratory, thereby remaining in complete darkness until completion of the scotopic phase of the ERG recordings. The ERG recording laboratory was completely light-proofed and accessed via the light-proofed ante-room.

2.5.1 | Induction of anaesthesia

Towards the end of the 2 h post-dose period, rats were anaesthetised using a combination of ketamine (Ketaset) 48 mg·kg^{-1} s.c. and medetomidine (Domitor) 0.5 mg·kg^{-1} s.c., to allow ERG recordings to begin approximately 2 h post-dose.

2.5.2 | Preparation of animals for ERG recordings

All experimentation was performed under dim red light (<2.4 log$_{10}$ nW·cm^{-2}, >650 nm). Pupil dilation was achieved through application of mydriatics (tropicamide 1% and phenylephrine 2.5%; Chauvin Pharmaceuticals, UK) to each eye. Hypromellose solution (0.5%; Alcon Laboratories, Ltd., UK) was also applied to each eye to retain corneal moisture and to provide sufficient adherence of a custom-made contact lens electrode (Sagdullaev, DeMarco, & McCall, 2004) to the corneal surface. A wire bite bar provided head support and acted as a ground, and a needle reference electrode (Ambu® Neuroline) was inserted approximately 5 mm from the base of the contralateral eye, sufficiently distal to exclude signal interference. Electrodes were connected to a Windows PC via a signal conditioner (Model 1902 Mark III, CED, UK) which differentially amplified (×3,000) and filtered (band-pass filter cut-off 0.5 to 200 Hz) the signal and a digitiser (Model 1401, CED). Throughout experimentation, core body temperature was maintained at ~37°C via a homeothermic heat mat (Harvard Apparatus, UK). For 10 min prior to first recordings, electrode stability was monitored and electrodes displaying any baseline instability were rejected.

2.5.3 | Scotopic (dark-adapted) ERGs

A xenon arc light source (Cairn Research Ltd.) connected to a ganzfeld sphere provided full-field white light flashes. The intensities of the ERG flash stimuli were measured using an optical power meter (PM203 Optical Power Meter; Macam Photometrics). To investigate the irradiance–response relationship of scotopic ERGs, light intensity was increased in a logarithmic scale using neutral density filters (Edmund Optics, UK) to provide corneal irradiances in the range of −4.9 to 3.1 log$_{10}$ μW·cm^{-2}. A series of 15 ms flashes were applied using an electrically controlled mechanical shutter (Cairn Research Ltd.). The inter-stimulus interval ranged from 1,500 ms at dimmest intensities to 30 s at brightest intensities. The number of stimuli was reduced from 30 to 6 at increasing intensities and an average trace was generated from recordings at each intensity.

2.5.4 | Photopic (light-adapted) ERGs

Cone photoreceptor activity was isolated via measure of responses to a bright white flash against a rod-saturating background light. Repeated bright white flashes (Grass Model PS33 Photic Stimulator, Astro-Med, Inc., Rhode Island, USA, fitted with a 400 nm high pass filter; 10 μs duration; peak corneal irradiance 3.3 $\log_{10}$ $\mu W \cdot cm^{-2}$) were applied at a frequency of 1.3 Hz against a rod-saturating, white background light (metal halide source; 2.8 $\log_{10}$ $\mu W \cdot cm^{-2}$). This was maintained over a period of 20 min and ERGs were recorded following each light pulse. Recordings were then grouped into sets of 25 and an average trace was generated for each set.

2.6 | Reversal and recovery from anaesthesia

The duration of anaesthesia was approximately 1 h for each rat. On completion of the recording, the contact lens electrode was carefully removed and "Tears Naturale" applied to the affected eye. The rats were then dosed with atipamezole (Antisedan) 0.5 $mg \cdot kg^{-1}$ s.c., to reverse the anaesthesia and placed on a warm surface in a recovery cage until deemed fit to return to the home cage. Animals were returned to their home cage between recordings. Where there was a requirement for >3 ERG recording sessions on separate occasions in individual rats (for the vehicle controls and 1,000 $mg \cdot kg^{-1}$ treatment group), the recording eye was alternated between sessions to facilitate recovery from any corneal surface irritation caused by the contact lens electrode.

2.7 | Test compounds

Three MCT1 inhibitors (AZD3965, AZ11709220 and AR-C117977XX) were evaluated (Murray et al., 2005; Påhlman et al., 2012; Curtis et al., 2017; Figure 1). The vehicle formulations used were water containing 0.5% w/v hydroxypropyl methylcellulose/0.1% w/v Tween 80 (AZD3965 and AZ11709220; both administered by oral gavage) or 5% w/v Tween 20 in saline (AR-C117977XX; subcutaneous injection). All three were tested using OptoMotry; doses were selected to provide maximal coverage of MCT1 in vivo. AZD3965 was also tested using ERG.

2.8 | ERG dosing and testing protocol

ERGs were performed prior to the onset of dosing to provide a predosing comparison (pretreatment). Animals were then dosed for a period of 7 days with either AZD3965 (1,000 $mg \cdot kg^{-1}$ p.o.) or its vehicle (10 $ml \cdot kg^{-1}$ p.o.). ERGs were performed at the following time points:- Day 1 (2 h post dosing); Day 7; Day 7 + 1; Day 7 + 4; Day 7 + 7. This scheme is summarised below.

To investigate the dose-dependent effects of AZD3965, ERGs were examined at Day 1 and Day 7 during a 7-day oral administration scheme for the following doses of AZD3965: 0 (vehicle), 10, 50, 200 and 1,000 $mg \cdot kg^{-1}$.

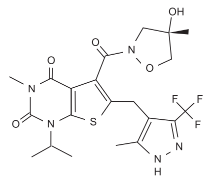

AZD3965

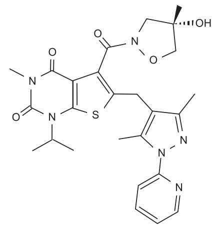

AZ11709220

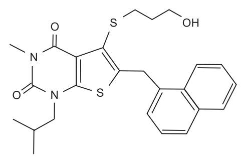

AR-C1197977XX

FIGURE 1 Molecular structures of the three MCT1 inhibitors evaluated

2.9 | Operational study design

For both the visual acuity and ERG components of the study, randomisation was achieved by allocating rats to treatment groups by body weight. Blinding procedures were not incorporated into the study design due to operational incompatibilities with the Good Laboratory Practice (GLP) compliance of the testing facility (standard operating procedures relating to cage labelling, animal identification, formulation labelling, dosing, study records and animal welfare checks). This is not considered to have significantly impacted on the outcome of the investigations in terms of introducing risk of intentional or unintentional bias, as the staff involved in the visual acuity recordings had no prior expectation of outcomes and the ERG recordings involve automated data acquisition. All group sizes were equal within each component of the investigation, with the exception of the visual acuity measurements in the AR-C117977XX study. In this case, there was a smaller number (5) in the vehicle control group than in the AR-C117977XX-treated group (8); this was considered acceptable due to the low variance in visual acuity measurements in vehicle control rats (Redfern et al., 2011). Otherwise, the design, data and statistical analysis comply with the recommendations on experimental design and analysis in pharmacology (Curtis et al., 2018) and with the ARRIVE Guidelines (Kilkenny et al., 2010).

2.10 | Data analysis and statistical analysis

The data and statistical analysis comply with the recommendations of the *British Journal of Pharmacology* on experimental design and analysis in pharmacology (Curtis et al., 2018). For visual acuity measurements after a single administration of compound in Han Wistar rats, Dunnett's test was used for AZD3965 and AZ11709220 (which both had three dose levels) and a Welch two-sample *t* test was used for AR-C117977XX (one dose level). Only decreases from vehicle control were considered likely (i.e., biologically plausible) for the visual acuity measurements, leading to a one-sided testing approach. AR-C117977XX was tested in male rats and was not accompanied by a measure of initial activity in the OptoMotry chamber. AZD3965 and AZ11709220 were each tested in equal numbers of male and female rats, and a measure of activity was included. The primary statistical analysis involved a comparison between the AZD3965- or AZ11709220-treated group and its vehicle control group in both females and males. The activity data were transformed using a square root transformation prior to analysis. A two-sided testing approach was used for activity as both increases and decreases from vehicle were possible. There was no statistically significant difference between males and females either in baseline measurements or in effects of different treatments. Also, there was no change in activity measured in the OptoMotry chamber in the evaluations of AZD3965 and AZ11709220.

For visual acuity measurements in the repeat-dose evaluation in Long-Evans rats, statistical objectives were to summarise the evidence of treatment related changes on visual acuity and activity in male and female animals. The primary measure of effect was selected to be the mean level on each day. The activity data were transformed using a square root transformation prior to analysis. Each parameter was analysed separately. The primary statistical analysis involved a comparison between the AZD3965-treated group and its vehicle control group in both females and males. Only decreases from vehicle control were considered likely for the visual acuity measurements, leading to a one-sided testing approach. A two-sided testing approach was used for activity as both increases and decreases from vehicle were possible. No adjustment for multiple testing was performed. In addition, comparisons between females and males in the two groups were also made using a two-sided testing approach for visual acuity and activity data. The statistical methods can be thought of as a series of *t* tests comparing either compound with vehicle or females with males on each day. In fact, a single model was used for each parameter, which is an improvement on such pairwise testing, as it takes advantage of the repeated measures on each animal to derive more robust estimates of the SEM changes. Technically, a random effects model was fitted with animal fitted as random. Group, sex and day were fitted as categorical variables and all three-way and two-way interactions between the factors were also fitted. A variance components covariance pattern structured by group was used. Differences in least square means (between test compound and vehicle groups or between females and males) were calculated.

For scotopic ERGs, the amplitude of the a-wave (from the stable baseline prior to stimulus onset, to a-wave peak) and the b-wave (from a-wave peak to b-wave peak) were measured for each data set. Sigmoidal curves were fitted to each dataset using GraphPad Prism v4 (Graphpad Software Inc, USA) using the following equation: $Y = V_{min} + (V_{max} - V_{min})/(1 + 10\text{^}((V_{50} - X)/\text{slope}))$. For photopic ERGs, due to low amplitude/undetectable a-waves, only b-wave amplitudes were measured for each data set. Two-phase exponential association curves were fitted to each data set using the following equation: $Y = Y_{max}1 \times (1 - e\text{^}(-K1 \times X)) + Y_{max}2 \times (1 - e\text{^}(-K2 \times X))$. To compare responses between groups, *F* tests were used to determine the best fit parameters and tested whether curves were statistically distinguishable ($P < 0.05$); one-way ANOVAs with Dunnett's post hoc test were used to compare response amplitudes between vehicle and 10–1,000 mg·kg^{-1} AZD3965 treated animals; two-way ANOVAs with Bonferroni post hoc test were used to compare response amplitudes between vehicle and 1,000 mg·kg^{-1} AZD3965 treated animals at different time-points. The post hoc tests were run only if *F* achieved $P < 0.05$ and there was no significant variance in homogeneity.

A *P*-value <0.05 versus vehicle control is considered to be statistically significant.

2.11 | Nomenclature of targets and ligands

Key protein targets and ligands in this article are hyperlinked to corresponding entries in the IUPHAR/BPS Guide to

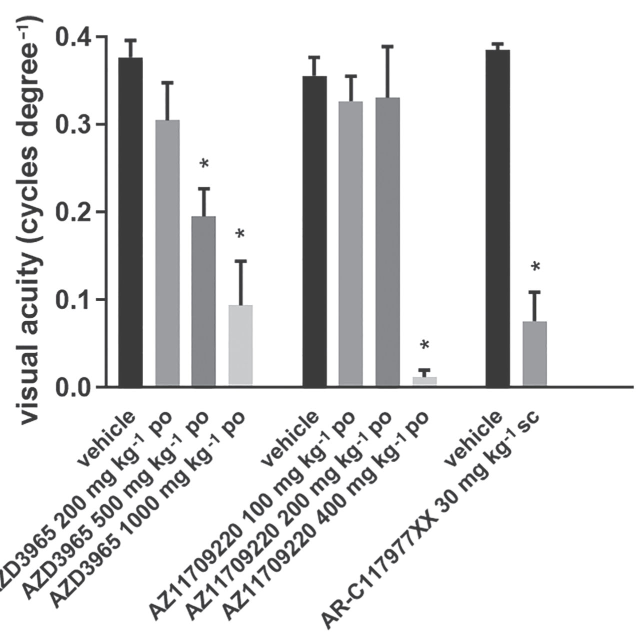

FIGURE 2 Effects of AZD3965 and two other MCT1 inhibitors on visual acuity measured using an optomotor reflex in Han Wistar rats. AZD3965, AZ11709220, and their vehicle control groups (three males and three females per group) were tested 1 h post-dose; AR-C1197977XX (eight males) and its vehicle control group (five males) were tested 2 h post-dose. Note that each of these MCT1 inhibitors decreased visual acuity when measured 1–2 h after a single dose. $^{*}P < 0.05$ compared to vehicle control group

PHARMACOLOGY http://www.guidetopharmacology.org and are permanently archived in the Concise Guide to PHARMACOLOGY 2019/20 (Alexander et al., 2019).

3 | RESULTS

3.1 | AZD3965 and two other MCT1 inhibitors decrease visual acuity after a single dose in albino (Han Wistar) rats

Figure 2 shows a decrease in visual acuity detected in conscious Han Wistar rats with three MCT1 inhibitors 1–2 h after administration. The key point here is not the magnitude of the effect (as the three compounds have differing potencies at MCT1, differing bioavailabilities and are likely to differ in their penetration of the blood-retinal barrier) but the finding that all three compounds were capable of producing a measurable deficit in visual acuity at their plasma T_{max} after a single administration. The effects of AZD3965 were dose-related.

3.2 | AZD3965 progressively decreases visual acuity on repeat-dosing in pigmented (Long Evans) rats

AZD3965 was evaluated in more detail at a single dose level (1,000 mg·kg^{-1} p.o.) in a 4-day repeat-dose study in Long Evans rats (Figure 3). Visual acuity in Long Evans rats is superior to Han Wistar rats (Douglas et al., 2005; Redfern et al., 2011) and this was also clearly evident in this study. The decrease in visual acuity following dosing with AZD3965 was far smaller than observed in the Han Wistar rats at the same dose level (1,000 mg·kg^{-1} p.o.). Plasma exposures were similar to those obtained at this dose level (1,000 mg·kg^{-1} p.o.) in Han Wistar rats (Table 1).

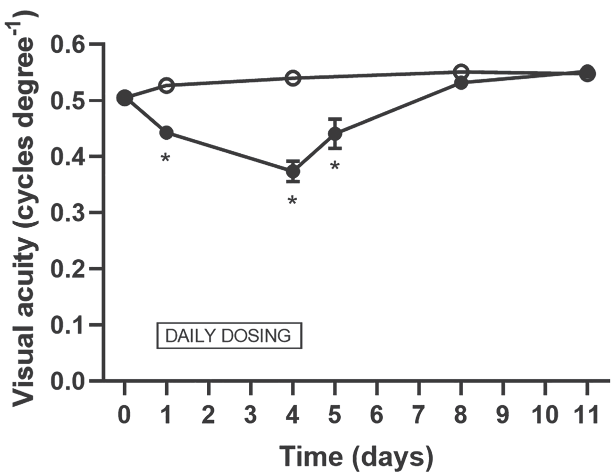

FIGURE 3 Time course of effects of effects of 4 days repeat-dosing with AZD3965 (1,000 mg·kg^{-1} p.o.) on visual acuity in Long Evans rats Dosing was for 4 days, with visual acuity measurements 1 h post-dose on Days 1 and 4, and on four subsequent occasions during the week after cessation of dosing. Open symbols: vehicle controls; filled symbols: AZD3965 1,000 mg·kg^{-1} p.o.; standard error bars are plotted but some are within the size of the symbols. Five males and five females per dose group (the data point on Day 5 was derived from the five males only and compared to the vehicle control data obtained on the previous day). Note the time-related decrease in visual acuity. This gradually recovered back to normal over the 7 days post-dosing. $^{*}P < 0.05$ compared to vehicle control group

3.3 | Assessment of potential confounding factors

The visual acuity measurement requires reflex head tracking in response to a moving grating and therefore is susceptible to other effects of test compounds, including effects on the level of arousal and on the general condition of the animals. Changes in the level of arousal could potentially impact on attention to the optomotor stimulus and/or on reflex head tracking behaviour. As a crude measure of activity, the number of times the "centring cross" was manually repositioned between the eyes by the observer in the first 60 s of the animal being placed in the OptoMotry chamber was logged. Compared to the vehicle controls, in Han Wistar rats, an approximately 50% increase in the activity measure was seen with AZD3965 at the highest dose tested only (1,000 mg·kg^{-1}; $P <.0.05$). Conversely, an approximately 40% decrease in the activity measure was seen with AZ11709220 at the highest dose tested only (400 mg·kg^{-1}; $P <.0.05$) These magnitudes of changes in activity are not considered to have accounted for the magnitude of the decreases in the visual acuity measure. The activity measure was not assessed in the case of AR-C117977XX as this compound was tested prior to our introduction of routine evaluation of activity in OptoMotry studies, but there were no clinical observations indicative of changes in the level of arousal. In the repeat-dose study with AZD3965 (1,000 mg·kg^{-1}) in Long Evans rats, there were no effects on the activity measure in the OptoMotry chamber at any time point nor was there any effect on condition of the animals or body weight gain.

3.4 | AZD3965 acutely impairs scotopic and photopic ERGs

Scotopic and photopic ERGs were recorded 2 h after receiving 0 (vehicle), 10, 50, 200 or 1,000 mg·kg^{-1} p.o. AZD3965. At doses of 50 mg·kg^{-1} p.o. and above, the scotopic ERG waveform was noticeably attenuated. This was reflected in low amplitude irradiance response curves of the b- and a-wave amplitudes (Figure 4b,c,e). No effect was apparent in rats dosed at 10 mg·kg^{-1} p.o. In contrast, significant effects of AZD3965 on the a-wave were only apparent at 1,000 mg·kg^{-1} p.o. At this dose level (1,000 mg·kg^{-1} p.o.), AZD3965 had marked effects on the scotopic ERG waveform across all intensities tested (Figure 4a). Indeed, all but one animal lacked a measurable b-wave at this time point, indicating that ON bipolar cell signalling and/or the photoreceptor: ON bipolar cell synapse is sensitive to MCT1 inhibition. Further quantification of these effects revealed a significant reduction in both b- and a-wave amplitudes (Figure 4c,e) that was not observed with vehicle-dosed animals (Figure 4c,e).

TABLE 1 Plasma exposure data for AZD3965 in the rat studies

	Day 1 μmol·L^{-1}	Day 4 μmol·L^{-1}	Day 6 μmol·L^{-1}
Han Wistar rats (visual acuity; M&F)			
200 mg·kg^{-1} p.o.	19.5 ± 9.1		
500 mg·kg^{-1} p.o.	**22.8 ± 6.4**		
1,000 mg·kg^{-1} p.o.	**30.8 ± 11.2**		
Long Evans rats (visual acuity; M&F)			
1,000 mg·kg^{-1} p.o.	**52.9 ± 7.2**	**63.5 ± 9.8**	
Long Evans rats (ERG; M)			
10 mg·kg^{-1} p.o.			1.5 ± 0.4
50 mg·kg^{-1} p.o.			**7.7 ± 2.2**
200 mg·kg^{-1} p.o.			**22.9 ± 4.4**
1,000 mg·kg^{-1} p.o.			**48.0 ± 7.3**

Note: Data presented are total plasma concentrations (mean ± *SD*) at 1 h 20 min post-dose (2 h post-dose for Day 4 of the repeat-dose visual acuity study in Long Evans rats). M male; F female. There were no sex differences in exposures (data not shown). Note that there is a small difference in exposure between the two strains of rat and no change in exposure on repeated dosing. Exposure data presented in bold were associated with statistically significant effects on visual acuity or electroretinogram (ERG) in their respective studies. Note that detectable effects on the ERG were observed at approximately threefold lower plasma concentrations than were effects on visual acuity. AZD3965 is approximately 64% unbound in plasma in the rat; therefore, the threshold total plasma exposure of 7.7 μmol·L^{-1} corresponds to a free plasma concentration of ~3 μmol·L^{-1}. The free concentration reaching the retina is unknown, but the expectation is that it would be at concentrations inhibiting MCT1 (nanomolar range) rather than MCT4 (inactive at 10 μM).

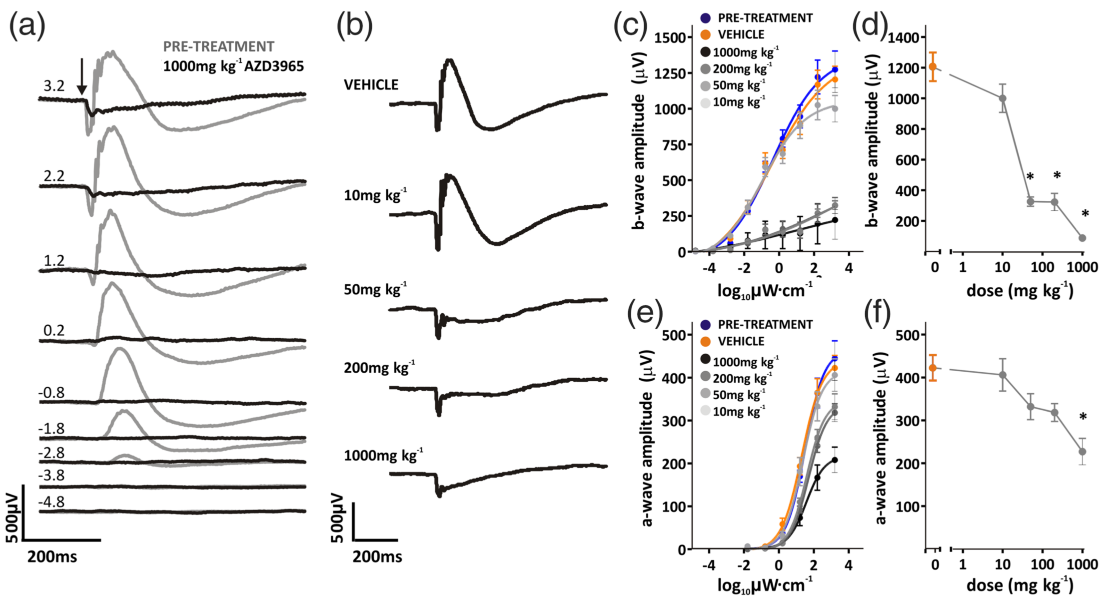

FIGURE 4 Acute effects of AZD3965 on dark-adapted ERG. (a) Representative dark-adapted (scotopic) ERG waveforms before (pretreatment; grey lines) and 2 h after (black lines) oral dosing with 1,000 mg·kg^{-1} AZD3965. Responses to increasing intensity stimuli are shown; number to left of traces indicates log intensity in μW·cm^{-2} (–4.8 to 3.2 $\log_{10}$ μW·cm^{-2}). Arrow indicates onset of 10 ms flash. (b) Representative ERG traces at 3.1 $\log_{10}$ μW·cm^{-2}, 2 h after oral dosing with vehicle, 10, 50, 200 or 1,000 mg·kg^{-1} AZD3965. Amplitudes of b-wave and a-wave to increasing light intensity flashes (–4.9 to 3.1 $\log_{10}$ μW·cm^{-2}) are shown in C&E, respectively, for before (pretreatment; blue) and 2 h after oral dosing with 10–1,000 mg·kg^{-1} AZD3965 (grey data points) or vehicle (orange). Dose-dependent differences are quantified in D&F, which displays b- and a-wave amplitudes to a 3.1 $\log_{10}$ μW·cm^{-2} flash for vehicle, 10, 50, 200 or 1,000 mg·kg^{-1} AZD3965 treated animals. Data presented are mean ± SEM, six animals per group. $^{*}P < 0.05$ compared to vehicle control group

A similar effect was apparent for photopic ERGs. Here, comparisons were made between b-wave amplitudes following 10 min of light adaptation, where significant effects of AZD3965 were apparent at doses of 50 mg·kg^{-1} p.o. and above (Figure 5).

Put together, these results indicate that doses of 50 mg·kg^{-1} p.o. AZD3965 and above have significant effects on retinal function as measured by the ERG, with a no-effect dose level of 10 mg·kg^{-1} p.o. The free plasma exposure at the threshold dose level (50 mg·kg^{-1}

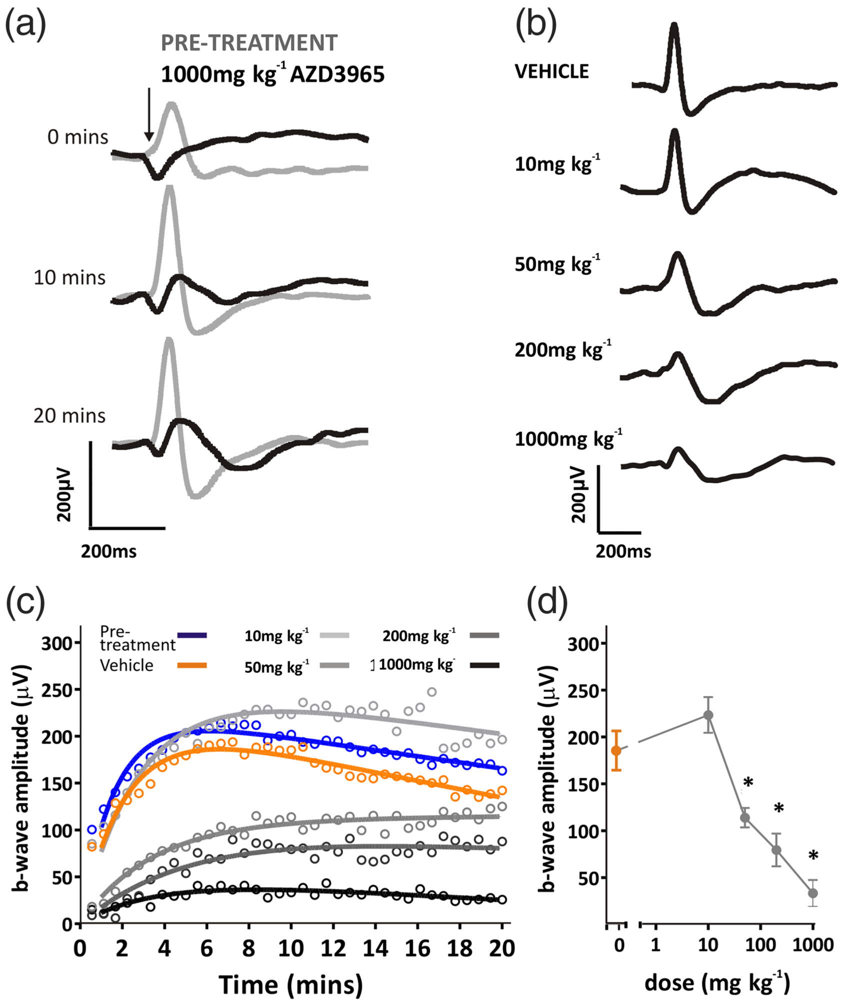

FIGURE 5 Acute effects of AZD3965 on light-adapted ERG. (a) Representative light-adapted (photopic) ERG waveforms before (pretreatment; grey lines) and 2 h after (black lines) application of 1,000 mg·kg^{-1} AZD3965. Responses are shown following 0, 10 and 20 min of a light-adapting background light; times are shown to the left of traces. Arrow indicates onset of 10 ms flash. (b) Representative ERG traces following 10 min light adaptation after 1 day dosing with vehicle, 10, 50, 200 or 1,000 mg·kg^{-1} AZD3965. Light-adapted b-wave amplitudes are shown in (c), before (pretreatment; blue) and 2 h after application of 10–1,000 mg·kg^{-1} AZD3965 (grey data points) or vehicle (orange). Note steady increase in b-wave amplitude for pretreatment and vehicle treated animals, indicating light-adaptation of retina. Dose-dependent differences are quantified in (d), which displays the b-wave amplitude after 10 min light adaptation for vehicle, 10, 50, 200 or 1,000 mg·kg^{-1} AZD3965 treated animals. Data presented are mean ± SEM. n = 6 for all groups. $^{*}P < 0.05$ compared to vehicle control group

p.o.) appears to accord with potency at MCT1 in vitro (Table 1). It is evident that both rod and cone retinal pathways are severely attenuated by MCT1 inhibition following high doses of AZD3965.

3.5 | ERG impairment attenuates during 7 days dosing of AZD3965

We were also interested to explore the effects of repeated dosing with AZD3965, given the marked effects of MCT1 inhibition on retinal function seen 2 h after dosing. Therefore, the effects of 7 days of repeated treatment with AZD3965 (10–1,000 mg·kg^{-1} p.o.) and subsequent recovery were examined (Figure 6). A degree of recovery was observed over 7 days treatment, so that only at doses of 1,000 mg·kg^{-1} p.o. were responses now significantly different from vehicle (Figure 6b–e). Likewise, light-adapted ERGs were now only significantly different from vehicle treated animals at doses of 200 mg·kg^{-1} p.o. and above (Figure 7). It seems that the effects of AZD3965 on retinal function show some alleviation over a period of 7 days dosing.

3.6 | ERG recovery after cessation of AZD3965 dosing

We compared scotopic and photopic ERGs after 7 days dosing with 1,000 mg·kg^{-1} p.o. AZD3965 or vehicle, and during the week following cessation of dosing. A noticeable recovery was apparent in ERG

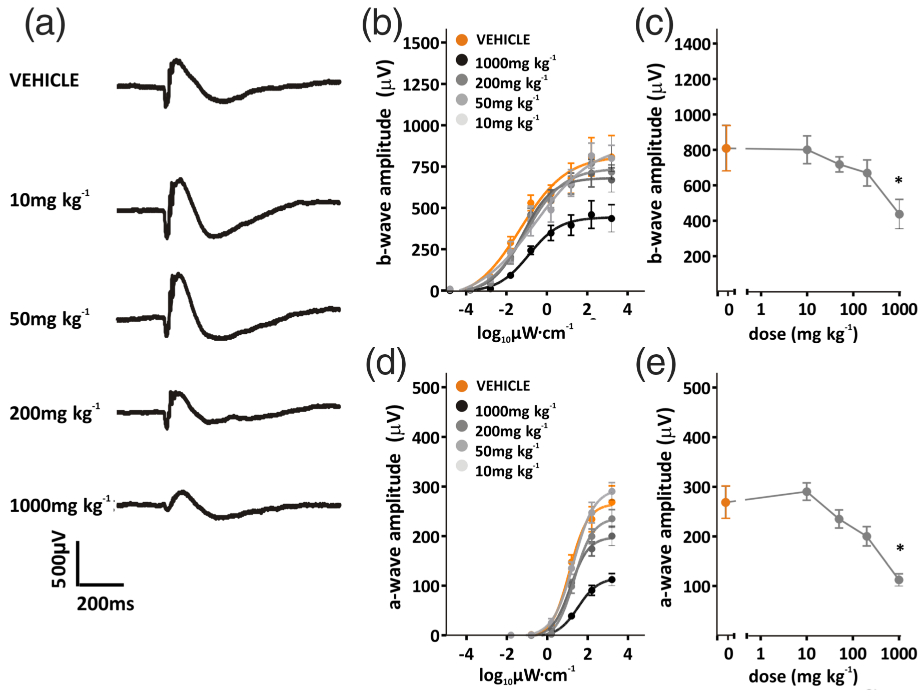

FIGURE 6 Dose–response curve for 7 days dosing of AZD3965: dark-adapted ERG (a), representative ERG traces at 3.1 $\log_{10}$ µW·cm^{-2}, after 7 days oral dosing with vehicle, 10, 50, 200 or 1,000 mg·kg^{-1} AZD3965. Amplitudes of b-wave and a-wave to increasing light intensity flashes (−4.9 to 3.1 $\log_{10}$ µW·cm^{-2}) are shown in (b) and (d), respectively, for animals dosed with vehicle (orange) or 10–1,000 mg·kg^{-1} AZD3965 (grey data points). Dose-dependent differences are quantified in (c) and (e), which display b- and a-wave amplitudes to a 3.1 $\log_{10}$ µW·cm^{-2} flash for vehicle, 10, 50, 200, or 1,000 mg·kg^{-1} AZD3965 treated animals. Data presented are mean ± SEM, n = 6 animals per group. $^*P < 0.05$ compared to vehicle control group

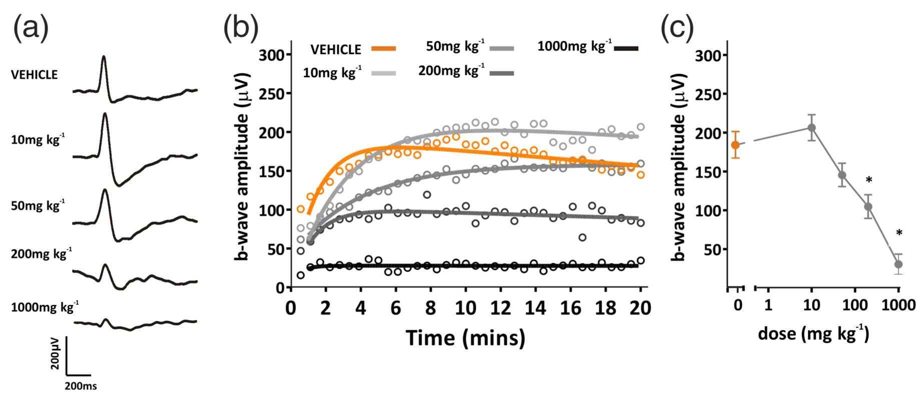

FIGURE 7 Dose–response curve for 7 days dosing of AZD3965: light-adapted ERG. (a) Representative ERG traces following 10 min light adaptation after 7 days oral dosing with vehicle, 10, 50, 200 or 1,000 mg·kg^{-1} AZD3965. (b) Light-adapted b-wave amplitudes for animals dosed with vehicle (orange) or 10 to 1,000 mg·kg^{-1} AZD3965 (grey data points). (c) b-wave amplitude after 10 min light adaptation for vehicle, 10, 50, 200 or 1,000 mg·kg^{-1} AZD3965 treated animals. Data presented are mean ± SEM. n = 6 for all groups. $^*P < 0.05$ compared to vehicle control group

waveforms over time (Figure 8a), that was mirrored in the recovery of b- and a-waves irradiance-response functions over time (Figure 8b,c). A comparison between 1,000 mg·kg^{-1} p.o. AZD3965 and vehicle treated animals over time in turn revealed recovery of b- and a-wave amplitudes by 7 days after cessation of dosing (day 7 + 7), so that no significant differences were apparent between 1,000 mg·kg^{-1} p.o. AZD3965 or vehicle treated animals (Figure 8d,e). An evaluation of the effects on oscillatory potentials showed a depression of the amplitude when assessed on day 7 of dosing, with a degree of recovery at day 7 + 7 (Figure 9a,b). Photopic ERGs also showed a degree of recovery in b-wave amplitude (Figure 10a,b), although responses remained significantly lower than vehicle treated animals at day 7 + 7 (Figure 10c). Thus, a more pronounced recovery of scotopic retinal function, compared with photopic function, was found.

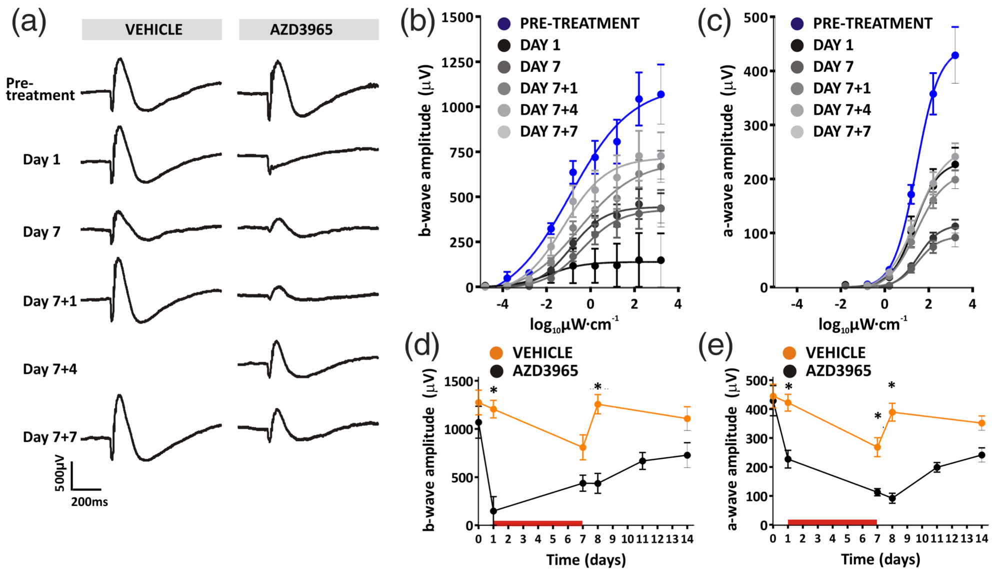

FIGURE 8 Long-term effects of 1,000 mg·kg^{-1} p.o. AZD3965 on dark-adapted ERG. (a) Representative ERG traces at 3.1 log$_{10}$ μW·cm^{-2} at time points before, during, and after dosing with vehicle (left panel) or 1,000 mg·kg^{-1} AZD3965 (right panel). These long-term effects are demonstrated in (b) and (c), which display b- and a-wave amplitudes, respectively, to increasing light intensity flashes (–4.9 to 3.1 log$_{10}$ μW·cm^{-2}) at time points before, during, and after dosing with 1,000 mg·kg^{-1} AZD3965. Time-dependent differences are quantified in (d) and (e), which show b-wave and a-wave amplitudes, respectively, for vehicle (orange) and 1,000 mg·kg^{-1} AZD3965 (black) treated animals. The red horizontal bar in (d) and (e) indicates the period of dosing. Data were compared with a two-way ANOVA, and differences between vehicle and AZD3965-treated animals were compared at individual time points using Bonferroni post hoc test. For b-wave: day 0, $P > 0.05$; day 1, $P < 0.05$; day 7, $P > 0.05$; day 7 + 1, $P < 0.05$; day 7 + 7, $P > 0.05$. For a-wave: day 0, $P > 0.05$; day 1, $P < 0.05$; day 7, $P < 0.05$; day 7 + 1, $P < 0.05$; day 7 + 7, $P > 0.05$. Data presented are mean ± SEM. $n = 6$ for all groups. $^*P < 0.05$ compared to vehicle control group

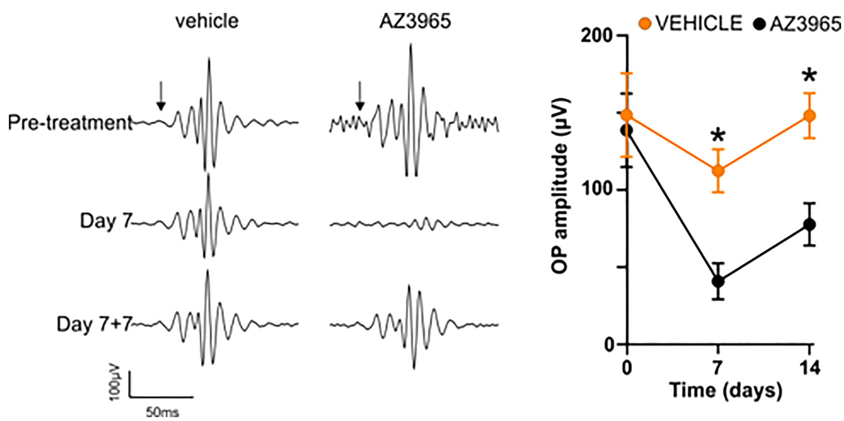

FIGURE 9 Long-term effects of 1,000 mg·kg^{-1} p.o. AZD3965 on oscillatory potentials of dark-adapted ERG. Left panel: representative recordings of oscillatory potentials prior to the start of the dosing phase, on Day 7 of dosing, and at 7 days after cessation of dosing with either vehicle or AZD3965 (1,000 mg·kg^{-1} per day). Right panel: Group mean data for oscillatory potential amplitude for 1,000 mg·kg^{-1} AZD3965 (grey data points) or vehicle (orange). Data were compared with a two-way ANOVA and differences between vehicle and AZD3965-treated animals were compared at individual time points using Bonferroni post hoc test. Day 0, $P > 0.05$; Day 7: $P < 0.05$; Day 14: $P < 0.05$. Data presented are mean ± SEM. $n = 6$ for all groups. $^*P < 0.05$ compared to vehicle control group

3.7 | Ophthalmology and retinal histopathology assessment

No retinal abnormalities were seen on ophthalmological examination and no histopathological changes were seen in the retinas of male and female Han Wistar rats dosed for 28 days with AZD3965 at doses up to 1,000 mg·kg^{-1} p.o. per day (unpublished AstraZeneca-generated data forming part of standard preclinical GLP regulatory submission).

4 | DISCUSSION

This study set out to characterise the effects of orally administered AZD3965, a potent and selective inhibitor of MCT1, on retinal and

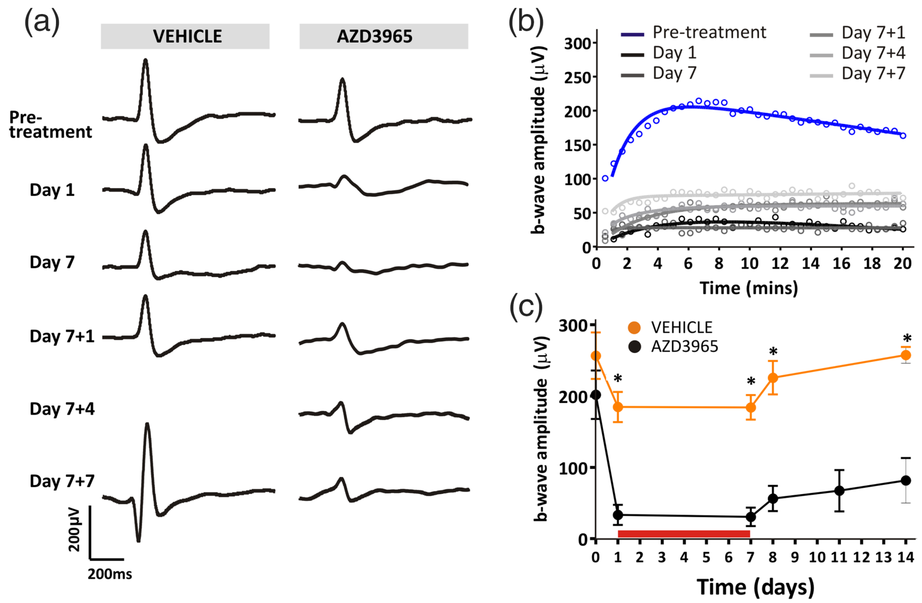

FIGURE 10 Long-term effects of 1,000 mg·kg^{-1} p.o. AZD3965 on light-adapted ERG. (a) Representative ERG traces following 10 min light adaptation at time points before, during, and after dosing with vehicle (left panel) or 1,000 mg·kg^{-1} AZD3965 (right panel). These effects are quantified in (b), which displays the change in b-wave amplitude over time for time points before, during, and after dosing with 1,000 mg·kg^{-1} AZD3965. These time-dependent differences are quantified in (c), which shows b-wave amplitude for vehicle (orange) and 1,000 mg·kg^{-1} AZD3965 (black) treated animals. The red horizontal bar in (b) and (c) indicates the period of dosing. Data were compared with a two-way ANOVA and differences between vehicle and AZD3965-treated animals were compared at individual time points using Bonferroni post hoc test. Day 0, $P > 0.05$; all other time-points, $P < 0.05$. Data presented are mean ± SEM. $n = 6$ for all groups. $^*P < 0.05$ compared to vehicle control group

visual function in the rat. Measurements of visual acuity in albino rats revealed deficits with AZD3965 after a single dose, a property in common with two other MCT1 inhibitors. On repeat-dosing in pigmented rats, AZD3965 (1,000 mg·kg^{-1} p.o.) caused a progressive deficit in visual acuity, which gradually recovered to pre-dose levels on cessation of dosing. At this high dose level (1,000 mg·kg^{-1} p.o.), the effects on visual acuity in pigmented rats were much smaller than in albino rats. Measurements of the electroretinogram (ERG) in pigmented rats revealed dose-related effects of AZD3965 on retinal function with evidence of reversibility, indicating that at appropriate doses, AZD3965 could be safely progressed into clinical development.

4.1 | Retinal functional effects of AZD3965

Detectable, dose-related effects of AZD3965 on the ERG were apparent as soon as 2 h after the first dose and at a dose level of 1,000 mg·kg^{-1} p.o. was manifested in the abolition of the b-wave and a small reduction in a-wave amplitude. The b-wave is classically associated with the depolarisation of ON bipolar cells, responding to a light-evoked decrease in photoreceptor glutamate release. As such, the responses we observed showed striking similarities to those observed during pharmacological blockade of the ON bipolar cell response (Massey, Redburn, & Crawford, 1983) or in mice lacking the glutamate receptor mGlu6 (Koyasu et al., 2008). Beyond this, however, defects in glutamate release from photoreceptor terminals, changes in synaptic architecture, the signalling complex of ON bipolar cells, ON bipolar cell degeneration and reductions in retinal perfusion, can also drive reductions in b-wave amplitude. The fact that we observed substantial recovery following cessation of dosing implies that these effects were unlikely to reflect retinal degeneration (which was confirmed as being absent in a 1-month repeat-dose toxicity study in the rat; AstraZeneca unpublished). Instead, it seems more plausible that MCT1 inhibition acts to alter glutamate signalling between photoreceptors and ON bipolar cells. This is also more easily reconciled with the relatively fast onset of effects observed here and in previous studies using nonselective MCT inhibitors such as 4-hydroxycinnamate and probenecid administered intravitreally (Bui, Kalloniatis, & Vingrys, 2004; Bui, Vingrys, et al., 2004) and the fact that 4-hydroxycinnamate drives decreases in retinal glutamate levels (Zeevalk & Nicklas, 2000). The plasma exposures of AZD3965 obtained over the dose range used (Table 1) were compatible with its selectivity for MCT1 over MCT4, especially when taking into account an expected (but unknown) reduction in tissue concentration at the level of the retina, due to the blood-retinal barrier (Hosoya & Tachikawa, 2009). However, an effect on MCT2 at higher dose levels cannot be ruled out.

If lactate is the primary substrate for retinal oxidative metabolism (Poitry-Yamate et al., 1995), MCT1 inhibition may well cause a widespread metabolic deficit in the retina, hindering normal energy-producing pathways. A compensatory mechanism for this has been suggested previously, in which retinal neurotransmitters including glutamate may be redirected to metabolic pathways to offset the lack of other metabolic substrates, such as lactate and pyruvate (Bui et al., 2009; Bui, Kalloniatis, & Vingrys, 2004; Bui, Vingrys, et al., 2004). Indeed, glutamate is understood to be an important metabolic substrate in other neuronal systems (Schousboe, 2017) and glutamate oxidation is known to elevate during energy deprivation (Bui, Vingrys, et al., 2004; Daikhin & Yudkoff, 2000). Thus, during a metabolic insult, photoreceptors might redirect glutamate to metabolic pathways in order to maintain normal photoreceptor function. This would explain why a much more subtle effect of AZD3965 was initially observed on photoreceptor function (as indicated by the a-wave). Moreover, this would ultimately reduce the glutamate available for neurotransmission and alter signalling between photoreceptors and bipolar cells, as indicated by the b-wave deficit.

There is increasing evidence that the b-wave is not merely a reflection of the ON bipolar-photoreceptor interaction and that third order, inner retinal neurones, particularly amacrine cells contribute to and modulate the b-wave (Dong & Hare, 2000, 2002; Möller & Eysteinsson, 2003). Thus, the effects observed on the ERG could be due to changes in amacrine activity to at least some extent. To address these issues would require examining the effects of MCT-1 inhibitors on individual neurones in the retinal network. Indirect evidence for an effect on amacrine cell function following repeated dosing with the high dose level of AZD3965 (1,000 $mg \cdot kg^{-1}$ p.o.) was provided by the observed reduction in the amplitude of the oscillatory potentials.

4.2 | Why did the ERG effect of MCT1 inhibition attenuate on repeated dosing?

There appeared to be an adaptive response of the retina to repeated dosing with AZD3965 over the 7-day period. This was not due to reduced plasma exposure. One such mechanism could be an up-regulation in the number of MCT1 transporters and/or of other MCT subtypes, in the cytoplasmic membrane and elsewhere in the cell. Another could be that, if the ERG effects were caused by "steal" of glutamate from the neurotransmitter pool, that this was restored by increased synthesis of glutamate. Alternatively, aspartate could be deployed as a substitute excitatory neurotransmitter. There is evidence for aspartate acting as an excitatory neurotransmitter in the brain (Cavallero, Marte, & Fedele, 2009), it is released in the brain when glutamate is depleted (Sonnewald & McKenna, 2002) and retinal aspartate levels increase in the rat retina after intravitreal injection of 4-hydroxycinnamate (Bui, Kalloniatis, & Vingrys, 2004). Further work would be required to uncover the mechanism of the adaptive response to prolonged inhibition of MCT1 in the retina.

4.3 | Why was this attenuation not seen with repeated dosing of AZD3965 on visual acuity?

Whereas the two types of assessment used (visual acuity and ERG) in the same strain of rat (Long Evans) both reported a functional deficit with AZD3965, the magnitude and time course of the effects were quite different. Interestingly, a larger effect on visual acuity was seen in albino rats at the same dose level, a phenomenon we have previously reported with the retinotoxic agent, sodium iodate (Redfern et al., 2011). The reasons for this are unknown but may be somehow related to the presence of **melanin** in the retina of pigmented animals. In pigmented (Long Evans) rats the ERG was more sensitive to the effects of AZD3965 than was visual acuity. This could imply a degree of redundancy in the retina in terms of functional deficits translating to effects on visual perception by the brain. Alternatively, whereas the ERG averages across the entire retina, it has been postulated that the optomotor reflex is predominantly triggered by image movement across the peripheral retina (Ueda, Nawa, Okamoto, & Hara, 2007). In the aforementioned study on sodium iodate, whereas the central retina was permanently damaged, the peripheral retina recovered and its recovery paralleled the time course of the restoration of the optomotor reflex (Redfern et al., 2011). Another difference between the two techniques is in the use of general anaesthesia for the ERG recordings. The optomotor reflex method of measuring rodent visual acuity is convenient, responsive to a wide range of drugs associated with retinal dysfunction (Maung et al., 2008) and can readily be incorporated into existing toxicology studies in rats without requiring additional animals or the use of anaesthesia (Redfern et al., 2013). It is best viewed as providing a *flag* for functional visual deficits caused by a test compound that would be followed up with an ERG study, which is more technically demanding, but is the acknowledged gold standard for assessing functional effects of drugs on the retina (Rosolen et al., 2005).

4.4 | Prediction of effects of AZD3965 on human vision prior to clinical trials

A reduction in ERG amplitude is generally associated with impaired vision in humans (Birch, 2004). It was therefore expected that the effects we observed following AZD3965 treatment in pigmented rats would be reflected in impaired visual function in human clinical trials. The precise nature of that effect, including whether it would be focal or global, was harder to predict. Nonetheless, a measurable b-wave was retained at all but the first timepoint at the highest dose in the rat ERG study and thus would be expected to preserve some vision. The reduced sensitivity of the scotopic ERG suggested that subjects may have reduced photosensitivity under night vision conditions. As we also observed clear drug effects on the photopic ERG in the rat, it seemed that daylight vision may also be affected.

4.5 | Effects of AZD3965 on ERG and vision in clinical trials: Evidence of good predictive translation

In the event, in the clinical trials thus far the patients have undergone ERG recordings and the maximum administered dose has been capped at a level where detectable changes begin to occur on the ERG

(Cancer Research, 2013; Plummer et al., 2017). Exclusion criteria included a history of retinal disease. The primary objectives were to determine the safety, dose-limiting toxicities and maximum tolerated dose of AZD3965. Intensive pharmacokinetic profiling was performed with subsequent modelling for receptor occupancy. Asymptomatic, reversible retinal ERG changes were first observed at 20 mg o.d. Several subjects were found to have reversible ERG changes, but with no discernible visual deficits (Plummer et al., 2017). This tallies with the rat data in that the ERG was more sensitive to the effects of AZD3965 than was visual acuity. The difference here was that the human subjects were not under anaesthesia for the ERG recordings, so anaesthesia was not a confounding factor. The main point is that there was good translation from rat to human for the ERG data; a more comprehensive PKPD comparison between rat and human will have to await publication of the clinical PK data. It should also be noted that in the rat we were able to explore dose levels up to 1,000 $mg{\cdot}kg^{-1}$, whereas the maximum dose level used in the human clinical trial (20 mg) is approximately equivalent to 0.3 $mg{\cdot}kg^{-1}$ (assuming a 70 kg human body weight).

Few drugs (of any pharmacological class) have been evaluated in both rat and human for their effects on ERG. Also, previous work on the pan-MCT inhibitors, 4-hydroxycinnamate and probenecid (Bui, Kalloniatis, & Vingrys, 2004; Bui, Vingrys, et al., 2004; Bui et al., 2009), has required intravitreal injections in rats (which would be unethical in humans).

5 | SUMMARY AND CONCLUSIONS

AZD3965, together with two other MCT1 inhibitors, caused a deficit in visual acuity in rats after a single administration. ERG studies in the rat confirmed that this was due to an effect on retinal function, with a decrease in b-wave amplitude the most obvious effect. The effects on the ERG occurred at lower plasma exposures than did the effects on visual function. On repeated dosing, the effects on visual function increased whereas the ERG effects attenuated. For both visual acuity and ERG, function was restored a few days after cessation of dosing. In clinical trials, ERG effects have been reported without effects on visual function. This study clarifies the role of the MCT1 transporter in retinal function and reveals good concordance between rat and human, indicating that the rat is an appropriate species for further research in this area that would yield findings of direct relevance to humans. The monitorability of its functional effects on the retina in the rat enabled safe clinical development of AZD3965 in oncology indications.

ACKNOWLEDGEMENTS

The authors wish to thank several current and former colleagues in AstraZeneca for their intellectual and operational support to this investigation: Mark Anderton, Lisa Burdett, Des Cobey, Susan Critchlow, Wendy Davies, Rowena Finney, Bryony Harrop, Natasha Karp, Richard Knight and Jean-Pierre Valentin.

AUTHOR CONTRIBUTIONS

A.E.A., E.A.M., R.J.L. and W.S.R. designed the investigations and prepared the manuscript. K.G. and C.G. conducted the visual acuity measurements. K.G. dosed and anaesthetised the animals for the ERG recordings. A.E.A. conducted the ERG recordings and analysis. P.V. ran the bioanalysis on plasma samples.

CONFLICT OF INTEREST

A.E.A. and R.J.L have no conflict of interest. E.A.M., W.S.R., K.G., C.G. and P.V. are or were employees of AstraZeneca plc at the time of the investigation.

DECLARATION OF TRANSPARENCY AND SCIENTIFIC RIGOUR

This Declaration acknowledges that this paper adheres to the principles for transparent reporting and scientific rigour of preclinical research as stated in the *BJP* guidelines for **Design and Analysis** and **Animal Experimentation**, and as recommended by funding agencies, publishers and other organisations engaged with supporting research.

DATA AVAILABILITY STATEMENT

All data were generated in a GLP-compliant facility, but GLP compliance was not claimed for these studies. Therefore, all data were acquired and recorded to GLP standards and are retrievable from secure archives. Advice from statisticians was sought before designing each of the component studies and in statistical analysis of the data.

ORCID

William S. Redfern https://orcid.org/0000-0001-7767-9515

REFERENCES

Alexander S. P. H., Kelly E., Mathie A., Peters J. A., Veale E. L., Armstrong J. F., … CGTP Collaborators (2019). THE CONCISE GUIDE TO PHARMACOLOGY 2019/20: Transporters. *British Journal of Pharmacology*, *176*(S1), S397–S493. https://doi.org/10.1111/bph.14753

Ames, A., Li, Y. Y., Heher, E. C., & Kimble, C. R. (1992). Energy metabolism of rabbit retina as related to function: High cost of Na^+ transport. *The Journal of Neuroscience*, *12*, 840–853. https://doi.org/10.1523/JNEUROSCI.12-03-00840.1992

Bergersen, L., Jóhannsson, E., Veruki, M. L., Nagelhus, E. A., Halestrap, A., Sejersted, O. M., & Ottersen, O. P. (1999). Cellular and subcellular expression of monocarboxylate transporters in the pigment epithelium and retina of the rat. *Neuroscience*, *90*, 319–331. https://doi.org/10.1016/S0306-4522(98)00427-8

Birch, D. G. (2004). Surrogate electroretinographic markers for assessing therapeutic efficacy in the retina. *Exp Rev Mol Diagnostics*, *4*, 693–703. https://doi.org/10.1586/14737159.4.5.693

Bröer, S., Bröer, A., Schneider, H. P., Stegen, C., Halestrap, A. P., & Deitmer, J. W. (1999). Characterization of the high-affinity monocarboxylate transporter MCT2 in Xenopus laevis oocytes. *The Biochemical Journal*, *341*, 529–535. https://doi.org/10.1042/bj3410529

Bröer, S., Schneider, H. P., Bröer, A., Rahman, B., Hamprecht, B., & Deitmer, J. W. (1998). Characterization of the monocarboxylate transporter 1 expressed in Xenopus laevis oocytes by changes in cytosolic pH. *The Biochemical Journal*, *333*, 167–174. https://doi.org/10.1042/bj3330167

Bui, B. V., Hu, R. G., Acosta, M. L., Donaldson, P., Vingrys, A. J., & Kalloniatis, M. (2009). Glutamate metabolic pathways and retinal function. *Journal of Neurochemistry*, *111*, 589–599. https://doi.org/10.1111/j.1471-4159.2009.06354.x

Bui, B. V., Kalloniatis, M., & Vingrys, A. J. (2004). Retinal function loss after monocarboxylate transport inhibition. *Investigative Ophthalmology & Visual Science*, *45*, 584–593. https://doi.org/10.1167/iovs.03-0695

Bui, B. V., Vingrys, A. J., Wellard, J. W., & Kalloniatis, M. (2004). Monocarboxylate transport inhibition alters retinal function and cellular amino acid levels. *The European Journal of Neuroscience*, *20*, 1525–1537. https://doi.org/10.1111/j.1460-9568.2004.03601.x

Cancer Research UK. (2013–18). A Phase I Trial of AZD3965 in patients with advanced cancer. https://clinicaltrials.gov/ct2/show/NCT01791595

Cavallero, A., Marte, A., & Fedele, E. (2009). L-Aspartate as an amino acid neurotransmitter: mechanisms of the depolarization-induced release from cerebrocortical synaptosomes. *Journal of Neurochemistry*, *110*, 924–934. https://doi.org/10.1111/j.1471-4159.2009.06187.x

Chidlow, G., Wood, J. P. M., Graham, M., & Osborne, N. N. (2005). Expression of monocarboxylate transporters in rat ocular tissues. *American Journal of Physiology. Cell Physiology*, *288*, C416–C428. https://doi.org/10.1152/ajpcell.00037.2004

Clem, B. F., O'Neal, J., Klarer, A. C., Telangand, S., & Chesney, J. (2016). Clinical development of cancer therapeutics that target metabolism. *QJM: An International Journal of Medicine*, *109*, 367–372. https://doi.org/10.1093/qjmed/hcv181

Curtis, M. J., Alexander, S., Cirino, G., Docherty, J. R., George, C. H., Giembycz, M. A., … Ahluwalia, A. (2018). Experimental design and analysis and their reporting II: Updated and simplified guidance for authors and peer reviewers. *British Journal of Pharmacology*, *175*, 987–993. https://doi.org/10.1111/bph.14153

Curtis, N. J., Mooney, L., Hopcroft, L., Michopoulos, F., Whalley, N., Zhong, H., … Critchlow, S. E. (2017). Pre-clinical pharmacology of AZD3965, a selective inhibitor of MCT1: DLBCL, NHL and Burkitt's lymphoma anti-tumor activity. *Oncotarget*, *8*, 69219–69236. https://doi.org/10.18632/oncotarget.18215

Daikhin, Y., & Yudkoff, M. (2000). Compartmentation of brain glutamate metabolism in neurons and glia. *The Journal of Nutrition*, *130*, 1026S–1031S. https://doi.org/10.1093/jn/130.4.1026S

Doherty, J. R., & Cleveland, J. L. (2013). Targeting lactate metabolism for cancer therapeutics. *The Journal of Clinical Investigation*, *123*, 3685–3692. https://doi.org/10.1172/JCI69741

Dong, C.-J., & Hare, W. A. (2000). Contribution to the kinetics and amplitude of the electroretinogram b-wave by third-order retinal neurons in the rabbit retina. *Vision Research*, *40*, 579–590. https://doi.org/10.1016/S0042-6989(99)00203-5

Dong, C.-J., & Hare, W. A. (2002). GABAc feedback pathway modulates the amplitude and kinetics of ERG b-wave in a mammalian retina in vivo. *Vision Research*, *42*, 1081–1087. https://doi.org/10.1016/S0042-6989(02)00032-9

Douglas, R. M., Alam, N. M., Silver, B. D., McGill, T. J., Tschetter, W. W., & Prusky, G. T. (2005). Independent visual threshold measurements in the two eyes of freely moving rats and mice using a virtual-reality optokinetic system. *Visual Neuroscience*, *22*, 677–684. https://doi.org/10.1017/S0952523805225166

Erecinska, M., & Silver, I. A. (1990). Metabolism and role of glutamate in mammalian brain. *Progress in Neurobiology*, *35*, 245–296. https://doi.org/10.1016/0301-0082(90)90013-7

Gerhart, D. Z., Leino, R. L., & Drewes, L. R. (1999). Distribution of monocarboxylate transporters MCT1 and MCT2 in rat retina. *Neuroscience*, *92*, 367–375. https://doi.org/10.1016/S0306-4522(98)00699-X

Grollman, E. F., Philp, N. J., McPhie, P., Ward, R. D., & Sauer, B. (2000). Determination of transport kinetics of chick MCT3 monocarboxylate transporter from retinal pigment epithelium by expression in genetically modified yeast. *Biochemistry*, *39*, 9351–9357. https://doi.org/10.1021/bi000464+

Halestrap, A. P., & Denton, R. M. (1975). The specificity and metabolic implications of the inhibition of pyruvate transport in isolated mitochondria and intact tissue preparations by alpha-Cyano-4-hydroxycinnamate and related compounds. *The Biochemical Journal*, *148*, 97–106. https://doi.org/10.1042/bj1480097

Halestrap, A. P., & Meredith, D. (2004). The SLC16 gene family-from monocarboxylate transporters (MCTs) to aromatic amino acid transporters and beyond. *Pflügers Archiv*, *447*, 619–628. https://doi.org/10.1007/s00424-003-1067-2

Halestrap, A. P., & Price, N. T. (1999). The proton-linked monocarboxylate transporter (MCT) family: structure, function and regulation. *The Biochemical Journal*, *343*, 281–299. https://doi.org/10.1042/bj3430281

Hosoya, K., Kondo, T., Tomi, M., Takanaga, H., Ohtsuki, S., & Terasaki, T. (2001). MCT1-mediated transport of L-lactic acid at the inner blood-retinal barrier: A possible route for delivery of monocarboxylic acid drugs to the retina. *Pharmaceutical Research*, *18*, 1669–1676. https://doi.org/10.1023/A:1013310210710

Hosoya, K., & Tachikawa, M. (2009). Inner blood-retinal barrier transporters: role of retinal drug delivery. *Pharmaceutical Research*, *26*, 2055–2065. https://doi.org/10.1007/s11095-009-9930-2

Jones, R. S., & Morris, M. E. (2016). Monocarboxylate transporters: Therapeutic targets and prognostic factors in disease. *Clinical Pharmacology and Therapeutics*, *100*, 454–463. https://doi.org/10.1002/cpt.418

Kenyon, E., Yu, K., La Cour, M., & Miller, S. S. (1994). Lactate transport mechanisms at apical and basolateral membranes of bovine retinal pigment epithelium. *The American Journal of Physiology*, *267*(6 Pt 1), C1561–C1573. https://doi.org/10.1152/ajpcell.1994.267.6.C1561

Kilkenny, C., Browne, W., Cuthill, I. C., Emerson, M., Altman, D. G., & NC3Rs Reporting Guidelines Working Group. (2010). Animal research: Reporting in vivo experiments: the ARRIVE guidelines. *British Journal of Pharmacology*, *160*, 1577–1579.

Koyasu, T., Kondo, M., Miyata, K., Ueno, S., Miyata, T., Nishizawa, Y., & Terasaki, H. (2008). Photopic electroretinograms of mGluR6-deficient mice. *Current Eye Research*, *33*, 91–99. https://doi.org/10.1080/02713680701823232

Lilley, E., Stanford, S. C., Kendall, D. E., Alexander, S. P., Cirino, G., Docherty, J. R., … Ahluwalia, A. (2020). *ARRIVE 2.0 and the British Journal of Pharmacology*: Updated guidance for 2020. *British Journal of Pharmacology*. https://doi.org/10.1111/bph.15178

Lin, H., La Cour, M., Andersen, M. V. N., & Miller, S. S. (1994). Proton-lactate cotransport in the apical membrane of frog retinal pigment epithelium. *Experimental Eye Research*, *59*, 679–688. https://doi.org/10.1006/exer.1994.1153

Manning Fox, J. E., Meredith, D., & Halestrap, A. P. (2000). Characterisation of human monocarboxylate transporter 4 substantiates its role in lactic acid efflux from skeletal muscle. *The Journal of Physiology*, *529*, 285–293.

Martinez-Outschoorn, U. E., Peiris-Pagès, M., Pesstell, R. G., Sotgia, F., & Lisanti, M. P. (2017). Cancer metabolism: A therapeutic perspective. *Nature Reviews Clinical Oncology*, *14*, 11–31. https://doi.org/10.1038/nrclinonc.2016.60

Massey, S. C., Redburn, D. A., & Crawford, M. L. (1983). The effects of 2-amino-4-phosphonobutyric acid (APB) on the ERG and ganglion cell discharge of rabbit retina. *Vision Research*, *23*, 1607–1613. https://doi.org/10.1016/0042-6989(83)90174-8

Maung, K. P., Storey, S., McKay, J., Bigley, A., Heathcote, D., Elliott, K., … Redfern, W. S. (2008). Validation of an optomotry system for measurement of visual acuity in Han Wistar rats. *Journal of Pharmacological and Toxicological Methods*, *58*, 152. https://doi.org/10.1016/j.vascn.2008.05.029

Möller, A., & Eysteinsson, T. (2003). Modulation of the components of the rat dark-adapted electroretinogram by the three subtypes of GABA receptors. *Visual Neuroscience*, *2003*(20), 535–542.

Murray, C. M., Hutchinson, R., Bantick, J. R., Belfield, G. P., Benjamin, A. D., Brazma, D., … Donald, D. K. (2005). Monocarboxylate transporter MCT1 is a target for immunosuppression. *Nature Chemical Biology*, *1*, 371–376. https://doi.org/10.1038/nchembio744

Påhlman, C., Zhongquan, Q., Murray, C. M., Ferguson, D., Bundick, R. V., Donald, D. K., & Ekberg, H. (2012). Immunosuppressive properties of a series of novel inhibitors of the monocarboxylate transporter MCT-1. *Transplant International*, *26*, 22–29.

Pellerin, L. (2003). Lactate as a pivotal element in neuron–glia metabolic cooperation. *Neurochemistry International*, *43*, 331–338. https://doi.org/10.1016/S0197-0186(03)00020-2

Percie du Sert, N., Hurst, V., Ahluwalia, A., Alam, S., Avey, M. T., Baker, M., … Würbel, H. (2020). The ARRIVE guidelines 2.0: Updated guidelines for reporting animal research. *PLoS Biology*, *18*(7), e3000410. https://doi.org/10.1371/journal.pbio.3000410

Philp, N. J., Wang, D., Yoon, H., & Hjelmeland, L. M. (2003). Polarized expression of monocarboxylate transporters in human retinal pigment epithelium and ARPE-19 cells. *Investigative Ophthalmology & Visual Science*, *44*, 1716–1721. https://doi.org/10.1167/iovs.02-0287

Philp, N. J., Yoon, H., & Grollman, E. F. (1998). Monocarboxylate transporter MCT1 is located in the apical membrane and MCT3 in the basal membrane of rat RPE. *The American Journal of Physiology*, *274*(6 Pt 2), R1824–R1828.

Plummer, R., Halford, S., Jones, P., Wedge, S., Hirschberg, S., Veal, G., … Banerji, U. (2017). A first-in-human first-in-class (FIC) trial of the monocarboxylate transporter 1 (MCT1) inhibitor AZD3965 in patients with advanced solid tumours. *Journal of Clinical Oncology*, *35*(15_suppl), 2516.

Poitry-Yamate, C. L., Poitry, S., & Tsacopoulos, M. (1995). Lactate released by Muller glial cells is metabolized by photoreceptors from mammalian retina. *The Journal of Neuroscience*, *15*, 5179–5191. https://doi.org/10.1523/JNEUROSCI.15-07-05179.1995

Polański, R., Hodgkinson, C. L., Fusi, A., Nonaka, D., Priest, L., Kelly, P., … Morrow, C. J. (2014). Activity of the monocarboxylate transporter 1 inhibitor AZD3965 in small cell lung cancer. *Clinical Cancer Research*, *20*, 926–937. https://doi.org/10.1158/1078-0432.CCR-13-2270

Prusky, G. T., Alam, N. M., Beekman, S., & Douglas, R. M. (2004). Rapid quantification of adult and developing mouse spatial vision using a virtual optomotor system. *Investigative Ophthalmology & Visual Science*, *45*, 4611–4616. https://doi.org/10.1167/iovs.04-0541

Redfern, W. S., Ewart, L. C., Lainée, P., Pinches, M., Robinson, S., & Valentin, J.-P. (2013). Functional assessments in repeat-dose toxicity studies: The art of the possible. *Toxicology Research*, *2*, 209–234. https://doi.org/10.1039/c3tx20093k

Redfern, W. S., Storey, S., Tse, K., Hussain, Q., Maung, K. P., Valentin, J.-P., … McKay, J. S. (2011). Evaluation of a convenient method of assessing rodent visual function in safety pharmacology studies: Effects of sodium iodate on visual acuity and retinal morphology in albino and pigmented rats and mice. *Journal of Pharmacological and Toxicological Methods*, *63*, 102–114. https://doi.org/10.1016/j.vascn.2010.06.008

Reichart, N., & Strauss, O. (2014). Ion channels and transporters of the retinal pigment epithelium. *Experimental Eye Research*, *126*, 27–37. https://doi.org/10.1016/j.exer.2014.05.005

Rosolen, S. G., Rigaudiere, F., Le Gargasson, J. F., & Brigell, M. G. (2005). Recommendations for a toxicological screening ERG procedure in laboratory animals. *Documenta Ophthalmologica*, *110*, 57–66. https://doi.org/10.1007/s10633-005-7344-y

Ross, S. J., & Critchlow, S. E. (2014). Emerging approaches to target tumor metabolism. *Current Opinion in Pharmacology*, *17*, 22–29. https://doi.org/10.1016/j.coph.2014.07.001

Sagdullaev, B. T., DeMarco, P. J., & McCall, M. A. (2004). Improved contact lens electrode for corneal ERG recordings in mice. *Documenta Ophthalmologica*, *108*, 181–184. https://doi.org/10.1007/s10633-004-5734-1

Schousboe, A. (2017). A tribute to Mary C. McKenna: Glutamate as energy substrate and neurotransmitter-functional interaction between neurons and astrocytes. *Neurochemical Research*, *42*, 4–9. https://doi.org/10.1007/s11064-015-1813-9

Selwan, E. M., Finicle, B. T., Kim, S. M., & Edinger, A. L. (2016). Attacking the supply wagons to starve cancer cells to death. *FEBS Letters*, *590*, 885–907. https://doi.org/10.1002/1873-3468.12121

Sonnewald, U., & McKenna, M. (2002). Metabolic compartmentation in cortical synaptosomes: Influence of glucose and preferential incorporation of endogenous glutamate into GABA. *Neurochemical Research*, *27*, 43–50. https://doi.org/10.1023/A:1014846404492

Sonveaux, P., Végran, F., Schroeder, T., Wergin, M. C., Verrax, J., Rabbani, Z. N., … Dewhirst, M. W. (2008). Targeting lactate-fueled respiration selectively kills hypoxic tumor cells in mice. *The Journal of Clinical Investigation*, *118*, 3930–3942. https://doi.org/10.1172/JCI36843

Tsacopoulos, M., & Magistretti, P. J. (1996). Metabolic coupling between glia and neurons. *The Journal of Neuroscience*, *16*, 877–885. https://doi.org/10.1523/JNEUROSCI.16-03-00877.1996

Tsacopoulos, M., Poitry-Yamate, C. L., MacLeish, P. R., & Poitry, S. (1998). Trafficking of molecules and metabolic signals in the retina. *Progress in Retinal and Eye Research*, *17*, 429–442. https://doi.org/10.1016/S1350-9462(98)00010-X

Ueda, T., Nawa, Y., Okamoto, M., & Hara, Y. (2007). Effect of pupil size on dynamic visual acuity. *Perceptual & Motor Skills*, *104*, 267–272. https://doi.org/10.2466/pms.104.1.267-272

Wang, L., Kondo, M., & Bill, A. (1997). Glucose metabolism in cat outer retina. Effects of light and hyperoxia. *Investigative Ophthalmology & Visual Science*, *38*, 48–55.

Wang, L., Tornquist, P., & Bill, A. (1997). Glucose metabolism of the inner retina in pigs in darkness and light. *Acta Physiologica Scandinavica*, *160*, 71–74. https://doi.org/10.1046/j.1365-201X.1997.00030.x

Winkler, B. S. (1981). Glycolytic and oxidative metabolism in relation to retinal function. *The Journal of General Physiology*, *77*, 667–692. https://doi.org/10.1085/jgp.77.6.667

Winkler, B. S., Pourcho, R. G., Starnes, C., Slocum, J., & Slocum, N. (2003). Metabolic mapping in mammalian retina: A biochemical and ^{3}H-2-deoxyglucose autoradiographic study. *Experimental Eye Research*, *77*, 327–337. https://doi.org/10.1016/S0014-4835(03)00147-7

Zeevalk, G. D., & Nicklas, W. J. (2000). Lactate prevents the alterations in tissue amino acids, decline in ATP, and cell damage due to aglycemia in retina. *Journal of Neurochemistry*, *75*, 1027–1034. https://doi.org/10.1046/j.1471-4159.2000.0751027.x

How to cite this article: Allen AE, Martin EA, Greenwood K, et al. Effects of a monocarboxylate transport 1 inhibitor, AZD3965, on retinal and visual function in the rat. *Br J Pharmacol*. 2020;177:4734–4749. https://doi.org/10.1111/bph.15239